SCIENTIFIC REPORTS

OPEN

SUBJECT AREAS:
HETEROGENEOUS CATALYSIS
SURFACE ASSEMBLY

Received
17 October 2014

Accepted
6 November 2014

Published
28 November 2014

Correspondence and requests for materials should be addressed to C.K.N. (narulack@ornl.gov)

Remarkable NO oxidation on single supported platinum atoms

Chaitanya K. Narula[1], Lawrence F. Allard[1], G. M. Stocks[1] & Melanie Moses-DeBusk[2]

[1]Materials Science & Technology Division, Oak Ridge National Laboratory, Oak Ridge, TN 37831-6133, [2]Energy & Transportation Science Division, Oak Ridge National Laboratory, Oak Ridge, TN 37831.

Our first-principles density functional theoretical modeling suggests that NO oxidation is feasible on fully oxidized single θ-Al_2O_3 supported platinum atoms via a modified Langmuir-Hinshelwood pathway. This is in contrast to the known decrease in NO oxidation activity of supported platinum with decreasing Pt particle size believed to be due to increased platinum oxidation. In order to validate our theoretical study, we evaluated single θ-Al_2O_3 supported platinum atoms and found them to exhibit remarkable NO oxidation activity. A comparison of turnover frequencies (TOF) of single supported Pt atoms with those of platinum particles for NO oxidation shows that single supported Pt atoms are as active as fully formed platinum particles. Thus, the overall picture of NO oxidation on supported Pt is that NO oxidation activity decreases with decreasing Pt particle size but accelerates when Pt is present only as single atoms.

Oxides of nitrogen (NO_X) are highly reactive gases that are emitted from cars, trucks and buses, power plants, and off-road equipment. These oxides contribute to ground level ozone and are known to have adverse effects on the human respiratory system. The abatement of nitrogen oxides generally involves an oxidation step to convert them all to NO_2 which can then be reduced to nitrogen with a reductant. Typically, a supported platinum catalyst is employed for the oxidation step[1–3], which is equilibrium limited over the temperature range of interest[4,5]. The weak and kinetically labile ON-O bond makes NO_2 even more effective at dosing a catalyst surface than O_2. This NO_2 dosing has been proposed to control platinum surface oxygen during NO oxidation[6–12]. The degree of surface oxygen coverage achieved during dosing and the oxygen binding energy depend on the concentrations of the reactants and products during the NO oxidation reaction. The dependence of NO oxidation on platinum particle size is well-known, with NO oxidation diminishing as the platinum particle sizes decrease[11]. Earlier studies failed to show if the cluster size effect is due to inactive Pt oxides or the presence of stronger surface Pt-O bonds in small clusters[11]. A recent detailed kinetic and isotopic study showed that large Pt clusters, which bind oxygen weakly as compared with smaller clusters, have higher vacancy concentrations and facile oxygen desorption[13]. First principles theoretical modeling of an NO interaction with a PtO_2 (110) surface shows that the surface has a weak ability to bind NO and O resulting in a high barrier (1.78 eV) for O_2 dissociation[14].

Since single supported atoms are the smallest possible clusters, it can be postulated that NO oxidation on such catalysts will be quite ineffective, especially since they are fully oxidized. However, supported single atom catalysts have generally been found to be more reactive than metal clusters or particles[15–22]. For example, the atomic dispersion of noble metal atoms was found to be the active species in the water-gas shift reaction[15]. Monodisperse palladium atoms on alumina, even at 0.03% loading, are highly active towards the selective oxidation of allylic alcohols[16]. Monodisperse single Pt atoms on iron oxide were shown to be highly active for CO oxidation and preferential CO oxidation in the presence of hydrogen[17]. Iridium single atoms on iron oxide exhibit high specific activity for the water gas shift reaction[18]. Monodisperse single Pt atoms on inert θ-alumina substrate are also highly active towards CO oxidation which occurs via a modified Langmuir-Hinshelwood (L-H) pathway[19]. Low temperature CO oxidation has been observed on single supported Pd atoms[20]. High catalytic activity of single supported silver atoms has been demonstrated by their ability to oxidize formaldehyde at low temperatures[21]. Finally, single atoms of rhodium are highly active toward methane reforming[22]. To our knowledge, there is no report describing NO oxidation on single supported atoms. It is important to point out that the study of NO oxidation on single atoms and rafts is relevant to NO_X abatement because single atoms and small rafts are present in fresh emission treatment catalysts along with well-defined Pt nanoparticles.

From a bonding perspective, NO bonded in a bent mode (M-N-O angle below 160°) to metals is considered to be NO^+ which is isoelectronic with CO. As such, we reasoned that NO oxidation can also occur via the modified L-H scheme proposed previously for single Pt atom catalyzed CO oxidation[19]. However, NO oxidation is

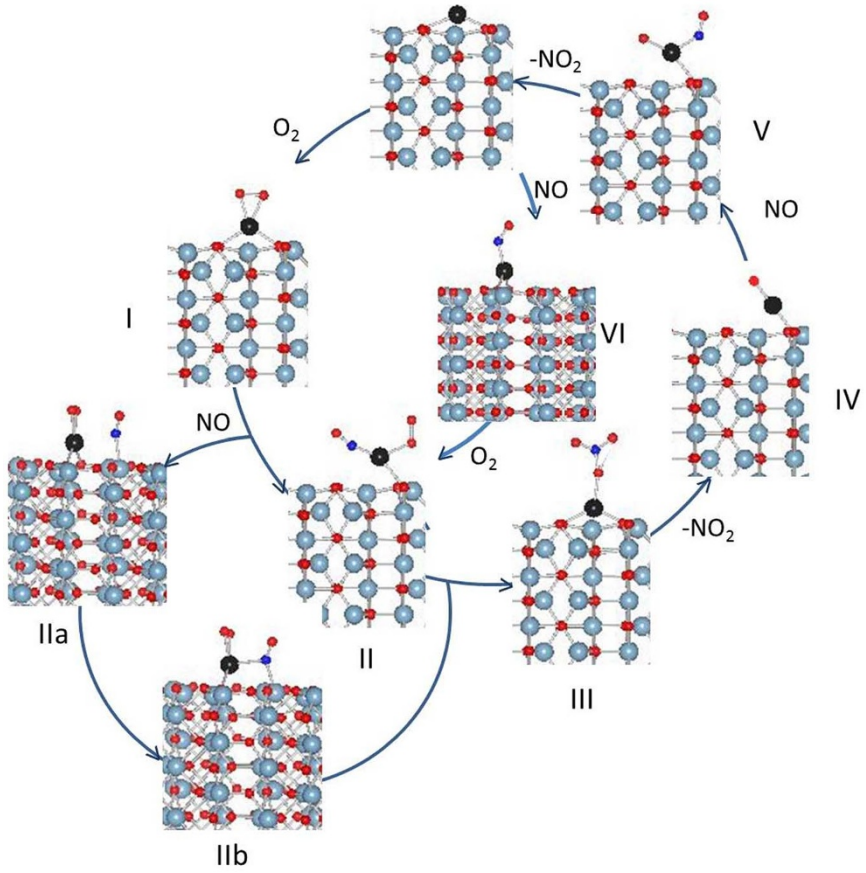

Figure 1 | Pathways for NO oxidation on single Pt atoms supported on the (010) surface of θ-Al_2O_3 [oxygen – red, aluminum – light blue, platinum – black, and nitrogen – blue].

complicated by the fact that it is less exothermic than CO as evident from a ΔH of reaction of −0.59 eV (cf. −2.93 eV for CO) and is equilibrium limited over the desired temperature range[4,5,23]. Thus, conclusions from the CO oxidation study are not applicable to NO oxidation[24]. Despite these considerations, our first principles study predicts that NO oxidation on single supported Pt atoms can proceed via a modified L-H mechanism. Our experimental work shows that single supported platinum atoms are indeed active for NO oxidation. The turnover frequency (TOF) of single supported Pt atoms is comparable to well-formed Pt particles. Thus, the overall picture of NO oxidation on supported Pt is that NO oxidation activity decreases with decreasing Pt particle size but accelerates when Pt is present only as single atoms or agglomerates of single atoms (e.g. rafts).

Results & Discussion

NO Oxidation Pathway on Single Pt Atoms on θ-Al_2O_3. The oxidation of NO on Pt (111) surfaces has recently been examined by Schneider et al[25]. Their results suggest that a high concentration of chemisorbed O is needed for NO oxidation on Pt but that the surface oxides are detrimental to reaction kinetics. O atoms were found to prefer FCC binding sites and arrange themselves to minimize destabilizing interactions with neighboring oxygens. Their results also show that the dissociative equilibrium of O_2(g) can produce coverage of up to ½ monolayer. The NO_2 decomposition or NO-assisted O_2 dissociation can increase coverage up to the $^2/_3$ monolayer normally observable during NO oxidation catalysis. Thus, Schneider et al. provide a useful guide via "Ellingham" free energy diagram of various oxidation reaction energies towards detailed reaction kinetics studies.

Unlike supported Pt particles, the single supported Pt atoms exist only as oxidized species under ambient or oxidizing conditions[19]. This implies that there is at least a monolayer coverage of oxygen on all single Pt atoms. The reduced form, where no oxygen is adsorbed on Pt atoms, can be stable as a transition state during a catalytic process[19,26]. For NO oxidation, the pathway shown in Figure 1 builds upon the recently published first-principles study of Pt atoms supported on the (010) surface of θ-Al_2O_3[25] and the proposed pathway for CO oxidation on supported Pt atoms[19].

The total energies of optimized species in Figure 1 are summarized in Table S1. The platinum atoms adsorb on the alumina surface in bridging positions between two oxygen atoms and are in a d^{10} oxidation state[26]. An oxygen molecule can bond to a Pt atom in a side-on chelating mode[19]. Unoccupied d_{xy} orbitals and the lack of magnetization support a d^8 structure for Pt atoms after oxygen bonding. Adsorption of NO on an oxidized Pt atom results in intermediate **II** [Figure 1]. NO bonds to Pt in a straight mode with a Pt-N-O angle of 163.8° suggesting a formal NO^- mode. Simultaneously, one of the Pt-O surface bonds breaks while the other surface Pt-O bond slightly lengthens by 0.06 Å to 2.248 Å. The side-on configuration of molecular oxygen also changes to terminal with a Pt-O bond of 2.06 Å. The magnetic moment is now localized completely on molecular oxygen suggesting a d^8 or d^{10} platinum species [Table S2]. The projected density of states orbital (PDOS) analysis shows partially filled d_{xy} and d_{x2} confirming a d^8 platinum [Figure S1].

We also explored an alternative pathway that involves NO bonded to aluminum adjacent to single Pt atoms. The NO molecule bonds to Al in a bent mode (Al-N-O angle of 139.8°) and the non-bonding Pt-N distance is 2.52 Å. The total energy of configuration **IIa** is −1339.1865 eV which is 1.84 eV higher than that of configuration **II**. In another possible configuration (**IIb**), which can form from either **IIa** or **I**, the NO molecule bonds to Al in a bent mode (Al-N-O angle of 132.56°) and bonds to Pt with Pt-N bond distance of

2.24 Å. The total energy of configuration **IIb** is −1339.2808 eV, which is also 1.75 eV higher than that of configuration **II**. These results suggest that NO oxidation can proceed on single supported Pt atoms without involving surface aluminum.

The rearrangement of **II** to a nitrate species in **III** is an endothermic step (1.09 eV). The nitrate species bonds to platinum in a mono-dentate mode. Such a mode has been previously observed for *trans*-Nitrato[2-(di-*tert*-butylphosphino)phenyl]-di-*tert*-butylphenylphosphine-platinum(II) with a Pt-O bond distance of 2.17 Å[27]. The calculated bond distance of Pt-O for the nitrate bonded to Pt in **III** is 2.09 Å. The platinum and all oxygen atoms on nitrogen carry a magnetic moment [Table S2], suggesting a d^9 oxidation state for Pt. The projected density of state analysis [Figure S2] shows $5d_{xy}$ is partially filled. The loss of NO_2 from **III** to form **IV** is also an endothermic process (1.24 eV). As described previously, **IV** is a high spin Pt species with partially filled Pt d_{xy} and d_{yz} orbitals[19]. The Pt-O bond distance with the remaining oxygen in **IV** contracts to 1.79 Å, while the Pt-O bond distances from surface oxygen become 0.2 Å larger suggesting a weaker support interaction than the non-oxidized platinum atom. The reaction of **IV** with NO to form **V** is an exothermic reaction. The Pt-N-O angle is 134.29° suggesting a formal NO^+ bonding mode (bent NO). The formation of the Pt-NO bond accompanies a break-up of one Pt-surface oxygen bond and lengthening of the other Pt-surface oxygen bond, suggesting a weakening of support interactions. Magnetization in intermediate **V** is on platinum, adsorbed oxygen, nitrogen and oxygen of adsorbed NO suggesting a d^9 platinum species. The PDOS analysis [Figure S3] shows partially filled d orbitals with vacancies in d_{xy} and d_{xz}. Elimination of NO_2 from **V** leads to a single supported Pt atom which restarts the NO oxidation cycle by oxygen adsorption. The NO adsorption is energetically less favorable than oxygen adsorption. The most favorable mode of NO adsorption is bent mode (Pt-N-O angle of 135.9°) shown in configuration **VI** in Figure 1. Other adsorption modes [Figure S4] did not optimize. In bent adsorption mode, the adsorption energy is −1.66 eV which is ~0.21 eV more than O_2 adsorption on single supported Pt atom in configuration **I**. Magnetization in intermediate **VI** is on platinum, nitrogen and oxygen of adsorbed NO suggesting a d^9 platinum species. The PDOS analysis [Figure S5] shows partially filled d orbitals with vacancies in d_{xy} and d_{xz}.

The energetics of reactions in Figure 1 can be summarized as presented in Table 1. The calculations in the table are based on total energies summarized in Table S1. All proposed reactions are energetically favorable except there is a barrier to nitrate formation and its decomposition. Thus, the first principles modeling results predicts that there is a pathway for NO oxidation on fully oxidized single supported Pt atoms. The experimental studies, described in the following paragraphs, show that single supported Pt atoms indeed catalyze NO oxidation.

NO Oxidation on θ-Al_2O_3 Supported Single Pt Atoms. The steady state NO oxidation on 0.18%Pt/θ-Al_2O_3 shows ~4% conversion at 265°C that increases only slightly to ~6% at 315°C but reaches ~15% at 415°C. This NO oxidation activity is much higher than that observed for blank θ-Al_2O_3 support [Figure S5]. Furthermore, the increase in activity is not related to platinum particle sintering as evinced from atomic imaging of the tested sample by aberration-corrected electron microscopy (ACEM) of 0.18%Pt/θ-Al_2O_3 after testing at all three temperatures, which showed predominantly well dispersed single atoms [Figure 2].

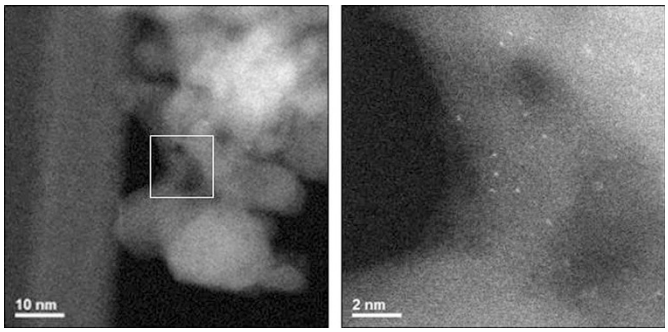

Figure 2 | ACEM, HAADF-STEM imaging of 0.18%Pt/θ-Al_2O_3, after NO oxidation testing up to 415°C. Low magnification (left) shows alumina and mono-dispersed Pt atoms can be seen at higher magnification (right). Image on right corresponds to white box area on left

For comparison, we also examined the NO oxidation activity of 2%Pt/θ-Al_2O_3 and 2%Pt_S/θ-Al_2O_3-650C keeping the surface Pt constant to limit NO oxidation variations to only Pt morphology variations. The 2%Pt/θ-Al_2O_3 catalyst contains 10–20 atom Pt rafts composed of Pt atoms that are not close enough for Pt-Pt bonding and are likely connected through Pt-O-Pt bonds[19]. The 2%Pt_S/θ-Al_2O_3-650C, on the other hand, contains primarily large particles[19]. The NO oxidation over 2%Pt/θ-Al_2O_3 at 265, 325, and 415°C is ca. 5, 10.5, and 17.5%, respectively and that over 2%Pt_S/θ-Al_2O_3-650C at 265, 325, and 415°C is ca. 7, 12, and 16%, respectively. These data show that the NO oxidation catalyzed by 2%Pt/θ-Al_2O_3 is comparable to that catalyzed by 0.18%Pt/θ-Al_2O_3 at 265°C but becomes more comparable to 2%Pt_S/θ-Al_2O_3-650C at 325 and 415°C, probably due to sintering. Sintering of Pt rafts to particles under NO oxidation condition has been previously reported[28]. The atomic imaging of the 2%Pt/θ-Al_2O_3 sample after testing confirms that some of the Pt rafts undergo sintering to ~5 nm particles although many rafts and some single atoms still remain in the sample [Figure S6]. For completeness, we also carried out NO oxidation over 2%Pt_T/θ-Al_2O_3-650C where total Pt content is identical to that of 0.18%Pt/θ-Al_2O_3. The NO oxidation over 2%Pt_T/θ-Al_2O_3-650C at 265, 325, and 415°C is 3, 7, and 11%, respectively.

The turn-over-frequencies (TOFs) at steady state for all catalysts are presented in Table 2. The TOFs were calculated using platinum distribution data[19] from fresh samples. This approach works well for samples of 0.18%Pt/θ-Al_2O_3 and 2%Pt_S/θ-Al_2O_3-650C since they do not change during NO oxidation. The TOF data for 2%Pt/θ-Al_2O_3 at 315°C and 415°C are estimates since some of the Pt in the sample undergoes sintering resulting in a reduced Pt dispersion. An interesting conclusion from TOF data is that the TOF of the single atoms in 0.18%Pt/θ-Al_2O_3 and the large particles in 2%Pt_S/θ-Al_2O_3-650C are comparable under the test conditions for NO oxidation at 415°C.

Table 1 | Energetics of Reactions in Figure 1

*Pt + O_2	= *Pt(O_2) (**I**)	−1.8736 eV
*Pt + NO	= *Pt(NO) (**VI**)	−1.6620 eV
*Pt(O_2) + NO	= *Pt(O2)(NO) (**II**)	−2.6238 eV
*Pt(O_2)(NO) (**II**)	= *Pt(NO_3) (**III**)	1.0912 eV
*Pt(NO_3) (**III**) - NO_2	= *Pt(O) (**IV**)	1.2400 eV
*Pt(O_2) (**IV**) - O	= *Pt(O) (**IV**)	5.6875 eV
*Pt(O) (**IV**) + NO	= *Pt(O)(NO) (**V**)	−2.5496 eV
*Pt(O)(NO) (**V**) – NO_2	= *Pt	1.3574 eV

The * represents the support.

Table 2 | TOF for NO Oxidation

Catalyst Samples	Pt_s	TOF (×10^{-4}/s)†		
	(mol)	265°C	315°C	415°C
0.18%Pt/θ-Al_2O_3	9.232e^{-7}	1.8	2.7	6.2
2.0%Pt/θ-Al_2O_3	9.232e^{-7}	2.0	4.2	7.1
2.0%Pt_S/θ-Al_2O_3-650C	9.232e^{-7}	2.9	4.7	6.6
2.0%Pt_T/θ-Al_2O_3-650C	4.613e^{-7}	2.7	5.7	10.1

†TOF was calculated based on Pt dispersion[22] [mol NOox/mol surface Pt (Pt_s)].

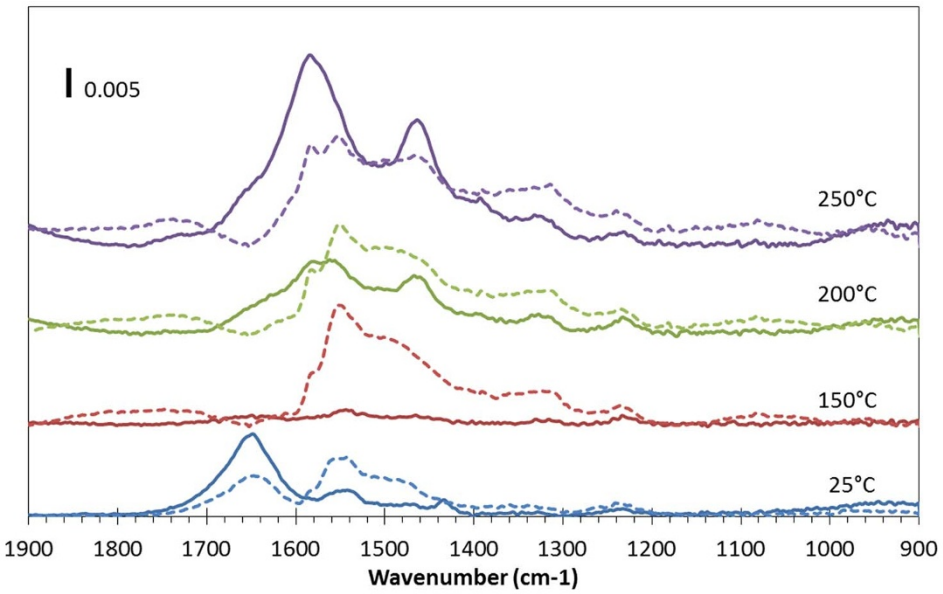

Figure 3 | DRIFTS of NO adsorption on alumina (dotted lines) and 0.18%Pt/θ-Al_2O_3 (solid lines) in 25–250°C range under NO.

Previous work in literature has shown that NO oxidation decreases with decrease in Pt particle[29,30]. The extrapolation of literature data suggests that TOF at single atoms would approach zero for NO oxidation. The high TOF on single supported Pt atoms could be due to a different pathway for NO oxidation.

The TOF of 2%Pt/θ-Al_2O_3 at 265°C is comparable to that of 0.18%Pt/θ-Al_2O_3 but becomes more comparable to 2%Pt/θ-Al_2O_3-650C at 315°C and 415°C due to Pt sintering. At 415°C, NO conversion of all three samples showed similar conversion and TOFs. The TOF of 2%Pt_S/θ-Al_2O_3-650C and 2%Pt_T/θ-Al_2O_3-650C were similar at 265°C when normalized for available surface Pt. However, by 315°C, the reduced number of available active sites in 2%Pt_T/θ-Al_2O_3-650C showed a slight improvement in intrinsic activity compared with 2%Pt_S/θ-Al_2O_3-650C which became more pronounced by 415°C (Table 2). This increase may be related to increased NO_2 inhibition on NO oxidation[9].

These results validate the proposal from theoretical modeling that single supported Pt atoms can catalyze NO oxidation.

Diffuse Reflectance Infra-Red Spectroscopy of NO adsorption on 0.18%Pt/θ-Al_2O_3. The role of the alumina support has been examined previously during NO oxidation and it has been found to be inactive toward NO oxidation[29]. An *in-situ* FTIR study has shown that NO or NO_2 adsorbs on alumina weakly at 250°C to form nitrates that desorb under a helium flush[16]. In the absence of oxygen, platinum supported on alumina also weakly adsorbs NO or NO_2 to form products that are identical to alumina except an additional nitrosium species (-NO-) is also observed[31]. The presence of oxygen in the reactant stream, on the other hand, dramatically increases NO_2 formation while the nitrosium species disappears[31]. Considering that NO oxidation over single supported Pt atoms cannot occur via conventional L-H scheme, we carried out diffuse reflectance Fourier transform spectroscopic study (DRIFTS) of NO adsorption in the absence and presence of oxygen over θ-Al_2O_3 and 0.18%Pt/θ-Al_2O_3.

The θ-alumina sample, at room temperature shows monodentate nitrate (asymmetric NO_2 stretch at 1550 cm^{-1} and symmetric NO_2 stretch at 1257 cm^{-1}) and linear nitrite as a shoulder at 1460 cm^{-1} [Figure 3][32]. There is also a peak at 1650 cm^{-1} due to residual bicarbonate which disappears upon increasing the temperature to 150°C and chelating nitrate (N = O stretch at 1590 cm^{-1} and asymmetric NO_2 stretch at 1305 cm^{-1}) appears[32]. In addition, a broad peak in 1650–1900 cm^{-1} is also observed which could have components of linear NO and residual gaseous NO. Increasing the temperature to 200 or 250°C does not significantly change the spectrum except nitrate and nitrite stretches become better defined. Exposure to NO and O_2 [Figure 4] at 250°C results in an increase in bands for chelating nitrate at 1590 cm^{-1} and monodentate nitrate at 1550 cm^{-1} is not separate. In addition, the broad band in 1650–1900 cm^{-1} narrows and is centered at 1732 cm^{-1} probably due to adsorbed linear NO. Increasing the temperature to 300°C leads to separation of bands for chelating and monodentate nitrate.

The spectrum of NO adsorbed on 0.18%Pt/θ-Al_2O_3 does not show a peak at 1727 cm^{-1} previously assigned to NO linearly bound to Pt at any temperature [Figure 3][33]. The residual bicarbonate peak at 1650 cm^{-1} seen for NO adsorption on θ-alumina was also observed on 0.18%Pt/θ-Al_2O_3 at 25°C and disappears on increasing the temperature. The peaks due to monodentate nitrate can be seen at 1550 cm^{-1}[32]. There is a unique band at 1432 cm^{-1} which can be assigned to non-coordinated carbonates. This band also disappears on increasing the temperature. At 200°C, the peaks due to monodentate and chelating nitrate are seen at 1550 and 1580 cm^{-1} and the peaks due to linear and bridging nitrite are seen at 1460 and 1314 cm^{-1}. Interestingly, the bent Pt-NO peak, reported in the literature to be present at 1630 cm^{-1} can be seen as a shoulder[33]. Increasing temperature to 250°C results in an increase in intensity of chelating nitrate peak at 1580 cm^{-1}. As a result, the monodentate nitrate peak and bent Pt-NO peak can be seen only as shoulders. A weak peak at ~1390 cm^{-1}, assignable to free nitrate, can also be observed. Exposure to NO + O_2 mixture [Figure 4] at 250°C results in monodentate and chelate nitrate peaks at 1550 and 1583 cm^{-1}, respectively, to be almost equal in intensity. In addition, the NO linear peak can be seen at 1735 cm^{-1}. Since Pt-free alumina shows this peak for both NO and NO + O_2 while 0.18%Pt/θ-Al_2O_3 exhibits it only for NO + O_2 gas mixture, we assign this peak to have a contribution of Pt-NO also.

Thus, the DRIFTS data clearly show that the primary differences between NO adsorption on supported Pt particles and single atoms is that the single atoms bond with NO only in bent mode in the absence of oxygen. The single supported Pt atoms are highly active towards NO oxidation since nitrate and nitrite peaks on Pt-containing alumina are much stronger than Pt-free alumina even in the absence of oxygen. This phenomenon has also been previously observed for alumina-supported Pt particles[32].

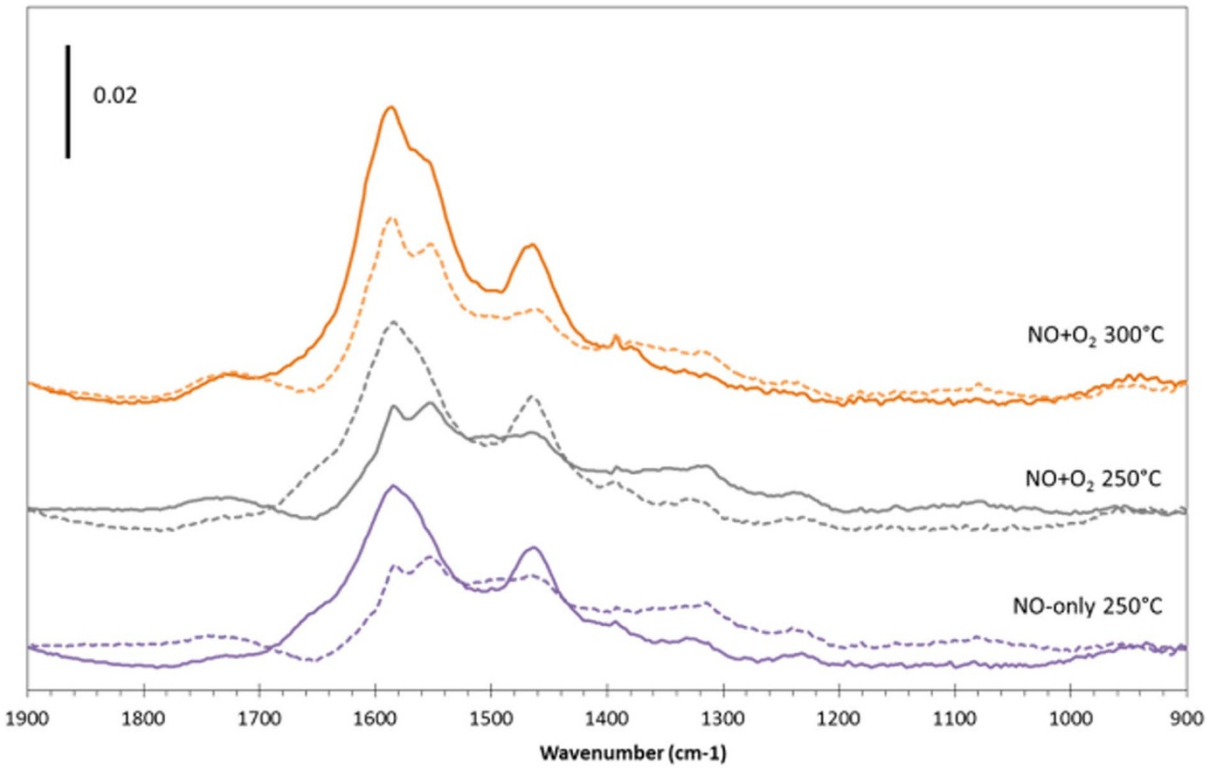

Figure 4 | DRIFTS of NO adsorption on alumina (dotted lines) and 0.18%Pt/θ-Al_2O_3 (solid lines) in 250–300°C range under NO + O_2.

The DRIFTS data are consistent with the proposed mechanism but the strong adsorptions of all species on alumina interfere with obtaining species bonded to Pt only. The absence of linear NO in 0.18%Pt/θ-Al_2O_3 when exposed to NO only is an indication that configuration **II** is not seen due to its transformation to nitrate. Since monodentate and chelating nitrate, bent NO, linear and bridging nitrite are also present in alumina, we refrain from using these observation in support of the proposed mechanism.

Conclusions

In conclusion, the results of first-principles theoretical modeling enable us to propose that NO oxidation on single supported platinum atoms is feasible although it is quite well known that NO oxidation decreases with decrease in particles size of supported Pt catalysts. The proposed pathway for NO oxidation is a modified L-H mechanism that does not involve the support and does not require dissociative oxygen adsorption. Experimental validation of our proposal comes from measuring the NO oxidation activity of single supported platinum atoms on an alumina catalyst, 0.18%Pt/θ-Al_2O_3. Imaging of the single-atom catalyst, 0.18%Pt/θ-Al_2O_3, after steady state testing from 265–415°C, shows that this supported Pt catalyst remains predominately single atoms.

The NO oxidation on 2%Pt/θ-Al_2O_3, containing 10–20 atom rafts, is similar to the supported single-atom catalyst but rapidly changes to mimic the large particle catalyst, 2%Pt/θ-Al_2O_3-650C, due to partial sintering of rafts. The lower TOF observed for 2%Pt/θ-Al_2O_3 compared to the pre-sintered Pt particles in 2%Pt/θ-Al_2O_3-650C at 315°C supports the well-known size dependent effect of the L-H mechanism.

Methods

Catalyst Preparation. The θ-Al_2O_3 support was prepared by a sol-gel process[34,35] and platinum samples [0.18% Pt/θ-Al_2O_3, 2.0% Pt/θ-Al_2O_3, and 2.0% Pt/θ-Al_2O_3-650C] were prepared by wet impregnation as reported previously[19]. All other materials were commercially available and used without further purification.

The 0.18%Pt/θ-Al_2O_3 catalyst consists of only single Pt atoms well dispersed on the alumina support[19]. The 2.0% Pt/θ-Al_2O_3 catalyst is composed of both single Pt atoms and 10–20 atom agglomerates, also referred to as platinum rafts bonded through oxygen (Pt-O-Pt)[19]. The 2.0% Pt/θ-Al_2O_3-650C catalyst sample is a pre-sintered version of the 2.0% Pt/θ-Al_2O_3 raft sample that was thermally treated at 650°C to produce a catalyst with predominately well-defined Pt particles[19].

Aberration-corrected high-resolution electron micrographs of catalyst samples were recorded on a JEOL 2200FS FEG 200 kv (scanning) transmission electron microscope (STEM), equipped with a CEOS GmbH (Heidelberg, Ger.) hexapole corrector on the probe-forming lenses. High-angle annular dark-field (HA-ADF) images showing single Pt atoms at a nominal resolution of 0.07 nm were collected at a 26.5 mr incidence semi-angle, using a detector having a 110 mr inner semi-angle.

In situ diffuse reflectance FT infrared spectroscopy (DRIFTS) measurement was performed on a Nicolet Nexus 670 spectrometer equipped with a MCT detector cooled by liquid nitrogen, and an *in situ* chamber (HC-900, Pike Technologies) with capability to heat samples to 900°C. The exiting stream was analyzed by an online quadrupole mass spectrometer (QMS) (OmniStar GSD-301 O2, Pfeffer Vacuum). All samples studied by DRIFTS were first heated to 150°C under a flow of 100 sccm of 4%H_2 in helium at a rate of 3°C/min and held at that temperature for 45 mins. The θ-Al_2O_3 sample was then cooled to 25°C under a flow of 100 sccm of helium. All spectra were obtained after exposure to 500 ppm NO in helium for 5 minutes. The sample was flushed with helium prior to temperature ramps under flowing helium. The 25°C spectrum of 0.18%Pt/θ-Al_2O_3 was obtained similar to the θ-Al_2O_3 sample. A second 0.18%Pt/θ-Al_2O_3 sample was reduced as described above without cooling. Instead the sample was flushed with helium at 150°C before exposure to the 500 ppm NO gas. The rest of the spectra were obtained from this second sample similar to the procedure previously described for θ-Al_2O_3. The oxidizing environment contained 500 ppm NO and 4.75% O_2. No helium flush was done at 250°C before exposure to the oxidizing flow or when ramping from 250 to 300°C. Space velocity conditions were kept constant from sample to sample. Each DRIFT spectrum was taken from a series recorded at a frequency of 16 scans per minute. The spectra presented in Figures 3 and 4 all had an automatic baseline correction applied for the reported 900–1900 cm^{-1} region.

NO Catalytic Activity Measurements. NO oxidation reactions were performed in a plug flow reactor and analyzed by a California Analytical, Inc. 400 HCLD NO_x analyzer. Powder catalyst samples were loaded in a U-tube quartz reactor between two quartz wool plugs. The catalyst temperature was monitored by a type *K* thermocouple positioned in the catalyst bed. The U-tube was heated in a reactor furnace controlled by another type *K* thermocouple located at the same height as the catalyst sample. In order to keep a constant gas hourly space velocity (GHSV) of ~55.5 k h^{-1}, the platinum catalysts were mixed with blank θ-Al_2O_3 to provide 120 mg test samples (0.108 mL) for all tests. The feed gas composition was 50 ppm NO, 1% O_2 and Ar as a balance. In order to achieve the low flow rate of O_2, a tank of zero air was used, introducing 3.76% N_2 into the total flow composition which was maintained at 100 sccm. The catalysts were heated to 120°C under argon before the

$NO + O_2$ reaction gas was introduced and the sample was further heated to the evaluation temperatures. Each sample was studied sequentially at the following set points: 270°C, 320°C and 420°C. The furnace was ramped at 4°C/min to 20°C below the set point and held for 5 min before ramping at 1°C/min for the final 20°C. The catalyst was held at the set point and allowed to stabilize for ~70 min before the NO_X concentration was averaged over 5 min. The analyzer was switched to NO mode and given 1–2 minutes to stabilize, and then the NO concentration was averaged over the next 5 min. The NO oxidation activity was calculated as $(NO_X - NO)/NO_X$. Catalyst comparisons were made keeping either the total platinum or surface platinum constant. TOF was calculated as moles of NO oxidized per mole of surface platinum (Pt_s) present in the fresh samples.

Computational Methods. The total energy calculations, based on ab initio density functional theory, were carried out employing the Vienna Ab Initio Simulation Package (VASP)[36]. A generalized gradient approximation (GGA) in the Perdew-Wang-91 form was employed for the electron exchange and correlation potential[37,38]. The projector-augmented wave (PAW) approach for describing electronic core states was employed to solve Kohn-Sham equations[39,40]. The plane wave basis set was truncated at a kinetic energy cutoff of 500 eV. As described previously, a Gaussian smearing function with a width of 0.05 eV was applied near Fermi levels. Ionic relaxations were considered converged when the forces on the ions were 0.03 eV/Å.

1. Shelef, M. & McCabe, R. W. Twenty five years after introduction of automotive catalysts: what next? *Catal. Today* **62**, 35–50 (2000).
2. Gandhi, H. S., Graham, G. W. & McCabe, R. W. Automotive exhaust catalysis. *J. Catal.* **216**, 433–442 (2003).
3. Jobson, E. Future challenges in automotive emission control. *Top. Catal.* **28**, 191–199 (2004).
4. Olsson, L. *et al.* A kinetic study of oxygen adsorption/desorption and NO oxidation over Pt/Al_2O_3 catalysts. *J. Phys. Chem. B* **103**, 10433–10439 (1999).
5. Olsson, L., Persson, H., Fridell, E., Skoglundh, M. & Andersson, B. A kinetic study of NO oxidation and NO_x storage on Pt/Al_2O_3 and $Pt/BaO/Al_2O_3$. *J. Phys. Chem. B* **105**, 6895–6906 (2001).
6. Bartram, M. E., Windham, R. G. & Koel, B. E. The molecular adsorption of nitrogen dioxide on Pt(111) studied by temperature programmed desorption and vibrational spectroscopy. *Surf. Sci.* **184**, 57–74 (1987).
7. Bartram, M. E., Windham, R. G. & Koel, B. E. Coadsorption of nitrogen-dioxide and oxygen on Pt(111). *Langmuir* **4**, 240–246 (1988).
8. Parker, D. H., Bartram, M. E. & Koel, B. E. Study of high coverages of atomic oxygen on the Pt(111) surface. *Surf. Sci.* **217**, 489–510 (1989).
9. Mulla, S., Chen, N., Deglass, W. N., Epling, W. S. & Ribeiro, F. H. NO_2 inhibits the catalytic reaction of NO and O_2 over Pt. *Catal. Lett.* **100**, 267–270 (2005).
10. Mulla, S. *et al.* Effect of potassium and water vapor on the catalytic reaction of nitric oxide and dioxygen over platinum. *Catal. Today* **114**, *114*, 57–63 (2006).
11. Mulla, S. *et al.* Reaction of NO and O_2 to NO_2 on Pt: Kinetics and catalyst deactivation. *J. Catal.* **241**, 389–399 (2006).
12. Smeltz, A. D., Getman, R. B., Schneider, W. F. & Ribeiro, F. H. Coupled theoretical and experimental analysis of surface coverage effects in Pt-catalyzed NO and O_2 reaction to NO_2 on Pt(111). *Catal. Today* **136**, *136*, 84–92 (2008).
13. Weiss, B. M. & Iglesia, E. NO oxidation catalysis on Pt Clusters: Elemntary steps, structural requirements, and synergistic effects of NO_2 adsorption sites. *J. Phys. Chem. C* **113**, 13331–13340 (2009).
14. Wang, H.-F., Guo, Y.-L., Lu, G. & Hu, P. NO oxidation on platinum group metal oxides: First principles calculations combined with microkinetic analysis. *J. Phys. Chem. C*, **113**, 18746–18752 (2009).
15. Fu, Q., Saltsburg, H. & Flytzani-Stephanopoulos, M. Active nonmetallic Au and Pt species on ceria-based water-gas shift catalysts. *Science* **301**, 935–938 (2003).
16. Hackett, S. E. J. *et al.* High-activity, single-site, mesoporous Pd/Al_2O_3 catalysts for selective aerobic oxidation of allylic alcohols. *Angew. Chem. Int. Ed.* **46**, 8593–8596 (2007).
17. Qiao, B. T. *et al.* Single atom catalysis of CO oxidation using $Pt1/FeO_x$. *Nat. Chem.* **3**, 634 (2011).
18. Lin, J. *et al.* Remarkable performance of Ir1/FeOx single-atom catalyst in water gas shift reaction. *J. Am. Chem. Soc.*, **135**, 15314–15317 (2013).
19. Moses-DeBusk *et al.* CO oxidation on supported single Pt atoms: Experimental and ab initio density functional studies of CO interaction with Pt atom on theta-Al_2O_3(101) surface. *J. Am. Chem. Soc.* **135**, 12634–12645 (2013).
20. Hu, P. *et al.* Electronic metal-support interactions in single-atom catalysis. *Angew. Chem. Int. Ed.* **53**, 3418–3421 (2014).
21. Peterson, E. J. *et al.* Low-temperature carbon monoxide oxidation catalyzed by regenerable atomically dispersed palladium on alumina. *Nature Comm.* **5**, 4885 (2014).
22. Duarte, R. B., Krumeich, F. & van Bokhoven, J. A. Structure, activity, and stability of atomically dispersed Rh in methane steam reforming. *ACS Catal.* **4**, 1279–1286 (2014).
23. Chemistry Webbook, Standard Reference Database Number 69. 2005.
24. Hong, S., Rahman, T. S., Jacobi, K. & Ertl, G. Interaction of NO with RuO_2(110) surface: A first principles study. *J. Phys. Chem. C* **111**, 12361–123681 (2007).
25. Getman, R. B., Xu, Y. & Schneider, W. F. Thermodynamics of environment-dependent oxygen chemisorption on Pt(111). *J. Phys. Chem. C* **112**, 9559–9572 (2008).
26. Narula, C. K. & Stocks, G. M. Ab Initio density functional calculations of adsorption of transition metal atoms on theta-Al_2O_3(010) surface. *J. Phys. Chem. C*, **116**, 5628–5636 (2012).
27. Countryman, R. & McDonald, W. S. *trans*-Nitrato[2-(di-*tert*-butylphosphino)phenyl]- di-*tert*-butylphenylphosphine-platinum(II). *Acta Cryst. B,* **33**, *33*, 3580–3581 (1977).
28. Narula, C. K., Allard, L. F., Blom, D. A. & Moses-DeBusk, M. Bridging the gap between theory and experiments – nanostructural changes in supported catalysts under operating conditions. *SAE Int. J. Mater. Manuf.* **1**, 182–188 (2009).
29. Xue, E., Seshan, K. & Ross, J. R. H. Role of support, Pt loading and Pt dispersion in the oxidation of NO to NO_2 and of SO_2 to SO_3. *Appl. Catal. B*, **11**, 65–79 (1996).
30. Matam, S. K. *et al.* The impact of aging environment on the evolution of Al_2O_3 supported Pt nanoparticles and their NO oxidation activity. *Appl. Chem. B* **129**, 214–224 (2013).
31. Captain, D. K. & Amiridis, M. D. *In situ* FTIR studies of the selective catalytic reduction of NO by C_3H_6 over Pt/Al_2O_3. *J. Catal.* **184**, 377–389 (1999).
32. Toops, T. J., Smith, D. B., Epling, W. E., Parks, J. E. & Partridge, W. P. Quantified NO_x adsorption on Pt/K/gamma-Al_2O_3 and the effects of CO_2 and H_2O. *Appl. Catal. B*, **58**, 255–264 (2005).
33. Chilukoti, S. *et al.* Spectral reconstruction of surface adsorbed species using band-target entropy minimization. Application to CO and NO reaction over a Pt/γ-Al_2O_3 catalyst using *in situ* DRIFT spectroscopy. *Phys. Chem. Chem. Phys.* **10**, 3535–3548 (2008).
34. Narula, C. K., Watkins, W. L. H. & Shelef, M. Aluminum oxide catalyst supports from alumina sols. *U.S. Patent no. 5*, 210,062 (1993).
35. Leenars, A. F., Keizer, K. & Burggraaf, A. The preparation and characterization of alumina membranes with ultra-fine pores. *J. Mater. Sci.* **19**, 1077–1088 (1984).
36. Kresse, G. Furthmuller, Efficiency of ab-initio total energy calculations for metals and semiconductors using a plane-wave basis set. *J. Comput. Mater. Sci.* **6**, 15–50 (1996).
37. Kresse, G. & Joubert, D. From ultrasoft pseudopotentials to the projector augmented-wave method. *Phys. Rev. B* **59**, 1758–1775 (1999).
38. Blochl, P E. Projector augmented-wave method. *Phys. Rev. B* **50**, 17953–17979 (1994).
39. Perdew, J. P. & Wang, Y. Accurate and simple analytic representation of the electron-gas correlation energy. *Phys. Rev. B* **45**, 13244–13249 (1992).
40. Perdew, J. P. *et al.* Molecules, solids, and surfaces: Applications of the generalized gradient approximation for exchange and correlation. *Phys. Rev. B* **46**, 6671–6687 (1992).

Acknowledgments

The research was sponsored by the U.S. Department of Energy, Office of Energy Efficiency and Renewable Energy, Vehicle Technologies Office, Propulsion Materials Program (C.K.N., M.M.D. L.F.A.) and Division of Materials Sciences and Engineering, Office of Basic Energy Sciences (G.M.S.) under contract DE-AC05-ooOR22725 with UT-Battelle, LLC. The DRIFTS studies were conducted at the Center for Nanophase Materials Sciences, which is sponsored at Oak Ridge National Laboratory by the Scientific User Facilities Division, Office of Basic Energy Sciences, U.S. Department of Energy.

Author contributions

C.N. developed the concept, carried out DFT calculations in collaboration with G.S., and wrote most of the paper. M.D. designed and carried out catalyst preparation, characterization, NO oxidation study including DRIFTS work, and wrote the experimental part in results and methods sections. L.A. conducted STEM examination of samples. All authors discussed the results, and commented on and edited the manuscript.

Additional information

Supplementary information accompanies this paper at http://www.nature.com/scientificreports

Competing financial interests: The authors declare no competing financial interests.

How to cite this article: Narula, C.K., Allard, L.F., Stocks, G.M. & Moses-DeBusk, M. Remarkable NO oxidation on single supported platinum atoms. *Sci. Rep.* **4**, 7238; DOI:10.1038/srep07238 (2014).